Foraminifers and conodonts in the Danlu section, South China: implications for the Viséan–Serpukhovian boundary (Mississippian)

Chao Liu[1] , Pedro Cózar[2], Ismael Coronado[3], Tian Liang[1], Xiaoxiao Liu[1],
Hao Chen[1], Xin Li[1], Haihua An[1] and Fukai Zhang[4]

[1]School of Resources and Environment, Henan Polytechnic University, Jiaozuo, China; [2]Instituto de Geociencias (CSIC-UCM), Madrid, Spain; [3]Facultad de Ciencias Biológicas y Ambientales, Universidad de León, León, Spain and [4]School of Software, Henan Polytechnic University, Jiaozuo, China

Abstract

The Viséan–Serpukhovian boundary is poorly defined in South China, hampering regional and global stratigraphical correlations. The foraminiferal and conodont distribution of the Baping Formation in the carbonate-slope Danlu section permits the recognition of an interval from the middle Viséan to the uppermost Serpukhovian in a continuous succession. The base of the Serpukhovian in Danlu is recognized by the first occurrences of *Janischewskina delicata*, *Howchinia subplana* and questionable '*Millerella*' *tortula*. At a slightly younger level, the conodont *Lochriea ziegleri* is first recorded. A calibration on the first occurrence of *L. ziegleri* in different basins at a global scale has been revised compared to auxiliary markers within the ammonoids and foraminifers. The late occurrence of *L. ziegleri* in the Danlu section also supports a lack of synchronicity in the global first occurrence of this taxon. This study calls for the recognition of a new base for the Serpukhovian under a far better correlation between different zonal schemes and fossil groups.

CAMBRIDGE
UNIVERSITY PRESS

1. Introduction

In the Carboniferous Period, the Viséan–Serpukhovian transition was proposed to coincide with the onset of the main cooling phase during the Late Palaeozoic Ice Age (LPIA) (Fielding *et al.* 2008; Montañez & Poulsen, 2013). This climate event, together with high-frequency glacioeustatic fluctuations, the Variscan Orogeny and closure of the equatorial Rheic seaway, resulted in pervasive discontinuous stratigraphical records and marine biotic provincialism worldwide (e.g. Nikolaeva & Kullmann, 2001; Korn *et al.* 2012; Wang *et al.* 2013; Davydov & Cózar, 2019). Due to a basin-wide unconformity coincident with the base of the Serpukhovian, the International Subcommission on Carboniferous Stratigraphy decided to search for a reliable faunal index to establish a Global Stratotype Section and Point (GSSP) close to the existing Viséan–Serpukhovian boundary (Richards & Task Group, 2003, 2005). Regional chronostratigraphy around this interval, mainly constructed with conodonts, foraminifers and ammonoids, was highly improved (e.g. Nikolaeva, 2013; Richards, 2013; Cózar & Somerville, 2014, 2016; Wang *et al.* 2018; Cózar *et al.* 2019; Nikolaeva *et al.* 2020), and the first appearance datum (FAD) of the conodont *Lochriea ziegleri* Nemirovskaya, Perret-Mirouse and Meischner in the lineage *L. nodosa* (Bischoff)–*L. ziegleri* is often considered to be the best marker for the new boundary definition (Richards & Task Group, 2005, 2014). This proposal is located at a slightly lower level than the traditional boundary in the Moscow Basin (Gibshman *et al.* 2009; Kabanov *et al.* 2016), but it still awaits official ratification, probably because the taxonomy of *L. ziegleri* and the isochronism of its first occurrence datum (FOD) in different basins need to be evaluated further (Sevastopulo & Barham, 2014; Barham *et al.* 2015; Herbig, 2017; Cózar *et al.* 2019).

The Naqing succession in South China contains the conodont lineage *L. nodosa–L. ziegleri* (Qi *et al.* 2014b) and was considered to be a suitable candidate for the Serpukhovian GSSP (Richards & Task Group, 2014). Unfortunately, this section yields no ammonoid and scarce representative foraminifers (Groves *et al.* 2012), making it difficult to calibrate the FOD of the *L. ziegleri* precisely (Cózar *et al.* 2019). Other carbonate-slope sections nearby, such as the Narao, Luokun and Dianzishang sections (Qi *et al.* 2014a; Wang *et al.* 2014; Sheng *et al.* 2021), provide little knowledge for the biostratigraphic calibration of the taxon as well.

Here, we present foraminiferal and conodont records of the Baping Formation in the Danlu section, Youjiang Basin, South China (Fig. 1). The aims are to (1) to calibrate the FOD of *L. ziegleri* in South China and (2) to assess the levels of diachronism of the FOD of *L. ziegleri* in different basins at a global scale.
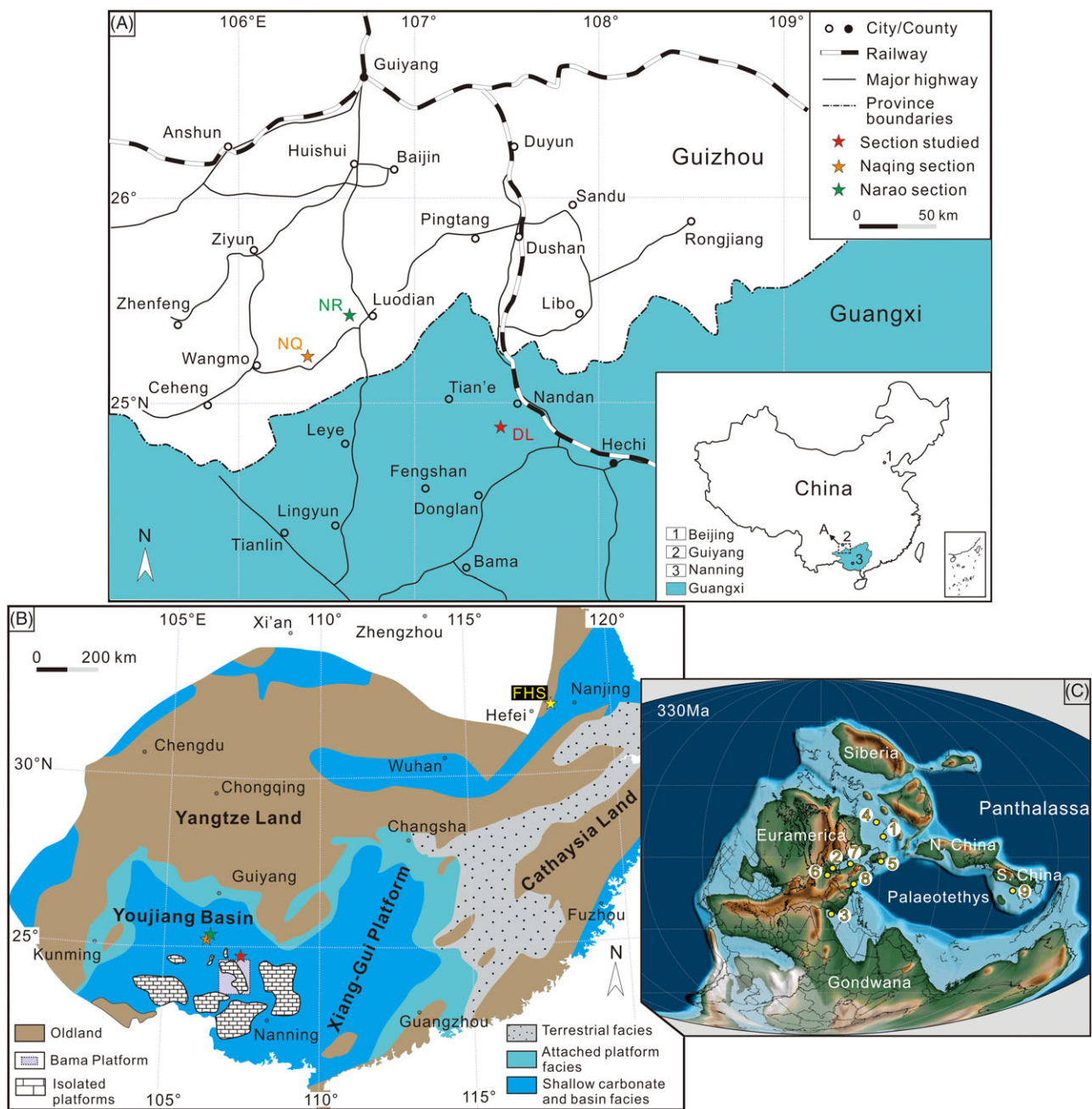
Fig. 1. (Colour online) Location map of the study area for the late Mississippian. (A) Index map showing the locations of the Danlu (DL), Naqing (NQ) and Narao (NR) sections. (B) Palaeogeographic map of South China (after Liu & Xu, 1994) and location of the Youjiang Basin and Bama Platform. Yellow star represents the Fenghuangshan section (FHS). (C) Global palaeogeographic reconstruction (modified from Scotese, 2021). Yellow dots point to approximate locations of the Danlu section and the referred sections beyond South China. 1, Urals; 2, northern England; 3, Cantabrian Mountains; 4, Moscow Basin; 5, Donets; 6, Ireland; 7, Germany; 8, NW Serbia; 9, Danlu. Other abbreviations: N./S. China, North/ South China.

2. Geological setting

During the late Mississippian, South China was situated within the eastern equatorial Palaeotethys (Fig. 1C). It mainly consists of the merged Yangtze and Cathaysia lands in the east, north and west, the attached platforms along the old land and the Xiang-Gui Platform and Youjiang Basin (also known as the Dian-Qian-Gui Basin or Nanpanjiang Basin) in the south (Fig. 1B) (Liu & Xu, 1994; Liu *et al.* 2015).

Cherts and volcanic rocks recorded in the succession suggest that the Youjiang Basin was a rift basin during the Devonian,

associated with the eastward expansion of the Palaeotethys (Du *et al.* 2013). Persistent rifting and subsidence during that time resulted in the development of two directional groups of faults (NW–SE and NE–SW), which regulated the palaeogeographic e- volution of the basin. Meanwhile, a number of tectonic blocks were detached from the southern margin of the Yangtze Land, giving rise to a submarine landscape composed of numerous iso- lated shallow-water carbonate platforms surrounded by basinal facies (Fig. 1B).

The Youjiang Basin evolved into a passive continental margin basin in the Mississippian, being tectonically quiescent for the

Pennsylvanian (Du *et al.* 2013). Most of the isolated platforms were gradually drowned during the late Permian to Early Triassic, due to a tectonic transition of the Youjiang Basin to a foreland setting (Liu *et al.* 2015).

Four lithofacies groups and depositional settings were mainly distinguished for the Mississippian in the Youjiang Basin by Qi *et al.* (2014b): (1) platform margin to slope facies with slumps and conglomerates; (2) platform margin with high-energy grainstones and reefs; (3) platform interior with low-energy shallow-marine carbonates and (4) shallow basins characterized by gravity flows.

The Bama Platform was one of such isolated platforms in the Youjiang Basin (Liu *et al.* 2015, 2023), and sections in the platform contain typical low-energy inner-platform carbonates (e.g. Gongchan and Shuidong) and platform marginal high-energy grainstones (e.g. Kacai). In contrast, the Danlu section (24° 49′44″ N, 107°28′24″ E) studied herein for the first time is located in Wuai Town, Nandan County (Fig. 1A) and preserves the late Mississippian carbonate-slope deposits of the Bama Platform (along the northern margin). From bottom to top, it comprises the Baping Formation and the lowermost Nandan Formation (Fig. 2). Lithologically, these rocks are comparable to the coeval deposits from the Naqing section (Qi *et al.* 2014b).

3. Sedimentology of the Danlu section

The Baping Formation (ca. 70 m thick) in the Danlu section, which underlies massive dolostones of the Nandan Formation (Pennsylvanian), is characterized by thin-bedded lime mudstones to wackestones intercalated with bioclast/intraclast-bearing packstones to grainstones (Fig. 2). Six lithofacies were separated, including lime mudstones to wackestones, laminated siltstones, bioclastic packstones and grainstones, normal-graded packstones to grainstones and massive dolostones.

Lime mudstones to wackestones are predominately thinly bedded and homogeneous, and in some cases weakly laminated or bioturbated. Radiolarian and sponge spicules are the most common components (Fig. 2G). Occasionally, this lithofacies is intercalated with laminated siltstones (Fig. 2E), or thin chert, shale, and peloidal packstone layers (Fig. 2G). Bioclastic packstones and grainstones mostly occur in the form of massive beds (up to 30 cm thick) and the contact with underlying mudstones to wackestones is irregular and sharp. Common carbonate grains incorporate foraminifers, crinoids, brachiopods and peloids (Fig. 2F). Although sharing some similarities with those bioclast-bearing limestones, normal-graded packstones to grainstones are distinguished by their normal-graded structure, thicker beds (ca. 40–120 cm), coarser grains and abundant poorly sorted irregular or abraded lithoclasts at the base (Fig. 2B, C). Massive dolostones capping the Baping Formation also exhibit the same features (Fig. 2H). These calcirudite-bearing beds occur in several intervals.

Common radiolarian and sponge spicules as well as rare bioturbation indicate that thin-bedded lime mudstones to wackestones were deposited in relatively deep-water conditions, below the storm wave base. Periodically concentrated normal-graded calcirudite-bearing beds, typically characterizing the base of turbidite sequences, are interpreted to be the result from turbidity currents on a slope environment during relative sea-level falls (Reijmer *et al.* 2012; Chen *et al.* 2016). Bioclast-bearing beds intercalated within muddy limestones were probably formed by distal turbidity currents during relative sea-level rises. Increased pressure on platform margin and upper slope sediment stack during transgression has been suggested to bring about debris flows with fine bioclasts into deeper settings (cf. Lantzsch *et al.* 2007). On this basis, six transgression–regression sequences can be recognized (Fig. 2). Thinning-upward cycles are usually documented in transgressive systems tracts (Fig. 2A). Location of the maximum flooding surfaces between transgressive and regressive systems tracts is difficult, and tentatively, they have been situated at the base of the calcirudite-bearing beds.

The Viséan–Serpukhovian boundary in the Danlu section coincides with a lithological change from a chert to a calcirudite-bearing bed between units 10 and 11 (Fig. 2D). The first *L. ziegleri* is yielded within a lime mudstone bed from the top of unit 11. The boundary and the FOD of *L. ziegleri* are both located at the uppermost regressive systems tract of Sequence 2 (Fig. 2).

4. Conodont distribution and biostratigraphy

Overall, the conodont fauna in the Danlu section is dominated by three genera, that is, *Gnathodus*, *Lochriea* and *Pseudognathodus* (Figs. 3, 4; Supplemental Appendix 2).

The base of the Danlu section mainly yields *Gnathodus bilineatus bilineatus* (Roundy) (Fig. 3B), *G. girtyi girtyi* Hass (Fig. 3D), *G. cantabricus* Belka & Lehmann, *G. homopunctatus* (Groessens & Noël), *G. semiglaber* Bischoff, *Pseudognathodus homopunctatus* (Ziegler) (Fig. 3E), *Lochriea commutata* (Branson & Mehl) (Fig. 3A) and *L. saharae* Nemyrovska, Perret-Mirouse and Weyant (Fig. 3C). This assemblage characterizes the *Gnathodus bilineatus* Zone from the basal Naqing section (Qi *et al.* 2014b; Hu *et al.* 2020). The index taxon for the *Lochriea nodosa* Zone was not found at Danlu, within this zone, but is first recorded much higher in the section. Nevertheless, as proposed by Qi *et al.* (2018), *L. costata* Pazukhin & Nemirovskaya first occurs only slightly later than *L. nodosa* in South China, though these two taxa, both derived from *L. commutata*, underwent distinct evolutionary lineages. The occurrence of *L. costata* at DL214 (Fig. 3F), in association with some species from underlying zones, can be thus regarded as an indicator for the *Lochriea nodosa* Zone (Fig. 4). The lower boundary of the *Lochriea ziegleri* Zone in the Danlu section is marked by the first *L. ziegleri* at DL224 (Figs. 3G, 4). Higher up in the section, apart from some long-ranging taxa (e.g. *L. nodosa* Nemirovskaya, Perret-Mirouse and Meischner; Fig. 3I), no new age-diagnostic element occurs (Fig. 4; Supplemental Appendix 2).

## 5. Foraminiferal distribution and biostratigraphy

Foraminifers are nearly absent in the basal part of the Danlu section (units 0 and 1; Fig. 4) because of the dominance of mudstones (Supplemental Appendix 1). The occurrence of *Endostaffella* suggests that it can be assigned to the middle Viséan (Cózar *et al.* 2022a) or the Tulian Russian Substage.

From unit 2, the assemblages change drastically, with more abundant and diverse foraminifers. It is noteworthy for the first occurrences of primitive *Neoarchaediscus* (e.g. *N.* aff. *parvus* (Rauser-Chernoussova); Fig. 5C, D), *Palaeotextularia* and *Archaediscus* spp. (at *angulatus* stage; Fig. 5B). Other important taxa in these levels are *Cribrospira mira* Rauser-Chernoussova, *Cribrostomum*, *Omphalotis* cf. *omphalota* (Rauser-Chernoussova & Reitlinger) and *Archaediscus* ex gr. *karreri* Brady (Fig. 5A). Higher up in unit 3, common *Pseudoendothyra*, *Endostaffella* (i.e. *E. parva* (Möller) and *E. shamordini* (Rauser-Chernoussova)), *Eostaffella proikensis* Rauser-Chernoussova (Fig. 5E) and the first representative of the genus '*Millerella*' occur
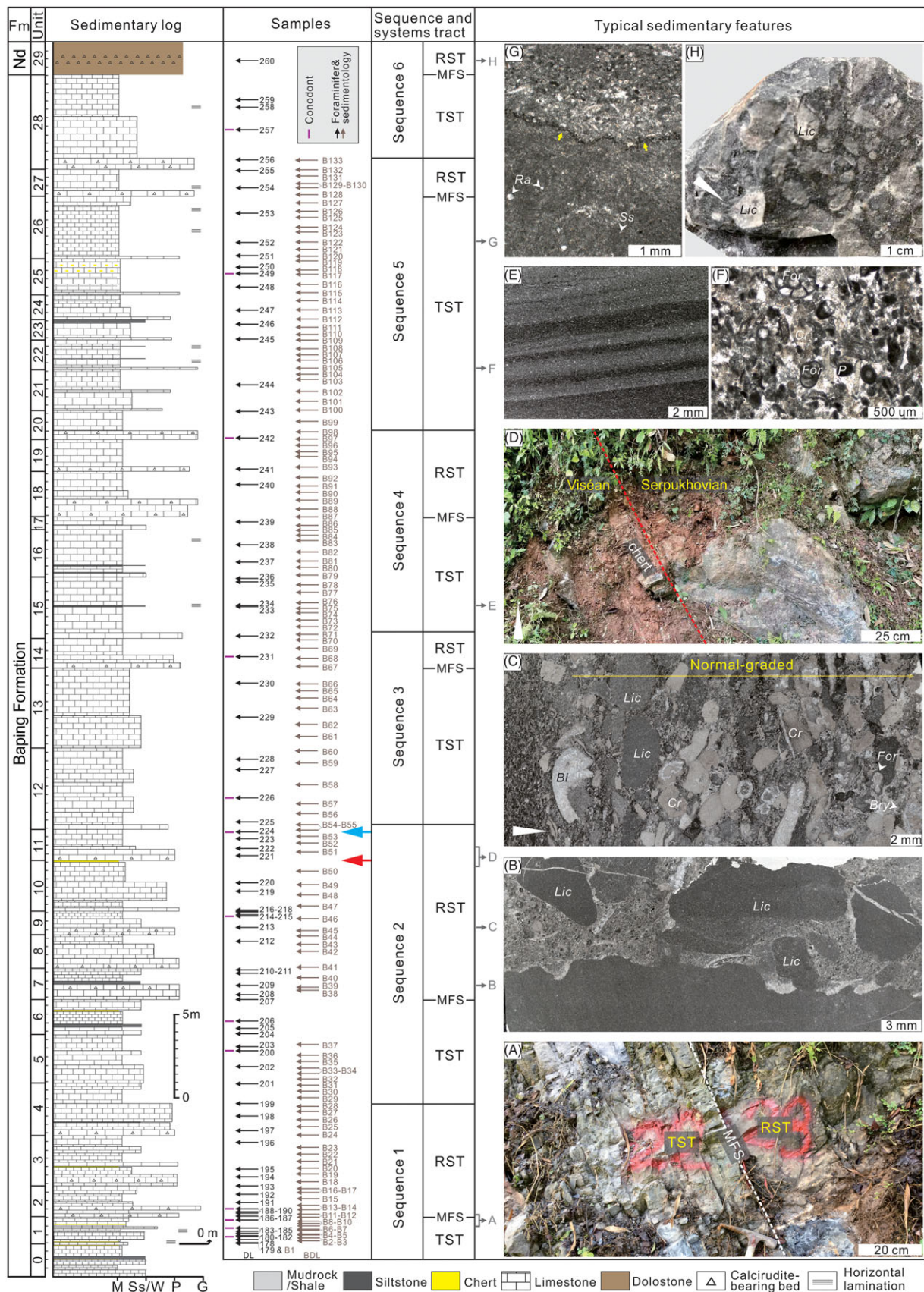
Fig. 2. (Colour online) Detailed sedimentary log, sampling, sedimentology-based sequence and systems tract interpretation of the Danlu section. Red arrow corresponds to the Viséan–Serpukhovian boundary defined by foraminifers and blue arrow to the FOD of *Lochriea ziegleri*. For the right column: (A) a representative of transgressive–regressive systems tract (TST–RST) transition, with maximum flooding surface (MFS) being the boundary; (B–C) coarse irregular or abraded litho-/bioclasts in normal-graded pack- to grainstones; (D) the Viséan–Serpukhovian boundary interval; (E) laminated siltstones; (F) fine bioclastic grainstones in a TST; (G) a peloidal packstone layer in thin-bedded lime mudstones with common radiolarians (*Ra*) and sponge spicules (*Ss*), and the contact is sharp and irregular (yellow arrows); (H) normal-graded dolostones with abundant cm-scale lithoclasts (*Lic*). Other abbreviations: Fm, Formation; Nd, Nandan Formation; M, lime mudstone or shale; Ss/W, siltstone/wackestone; P, packstone; G, grainstone; *Bi*, bivalve; *Cr*, crinoid; *For*, foraminifer; *Bry*, bryozoan; *P*, peloid.
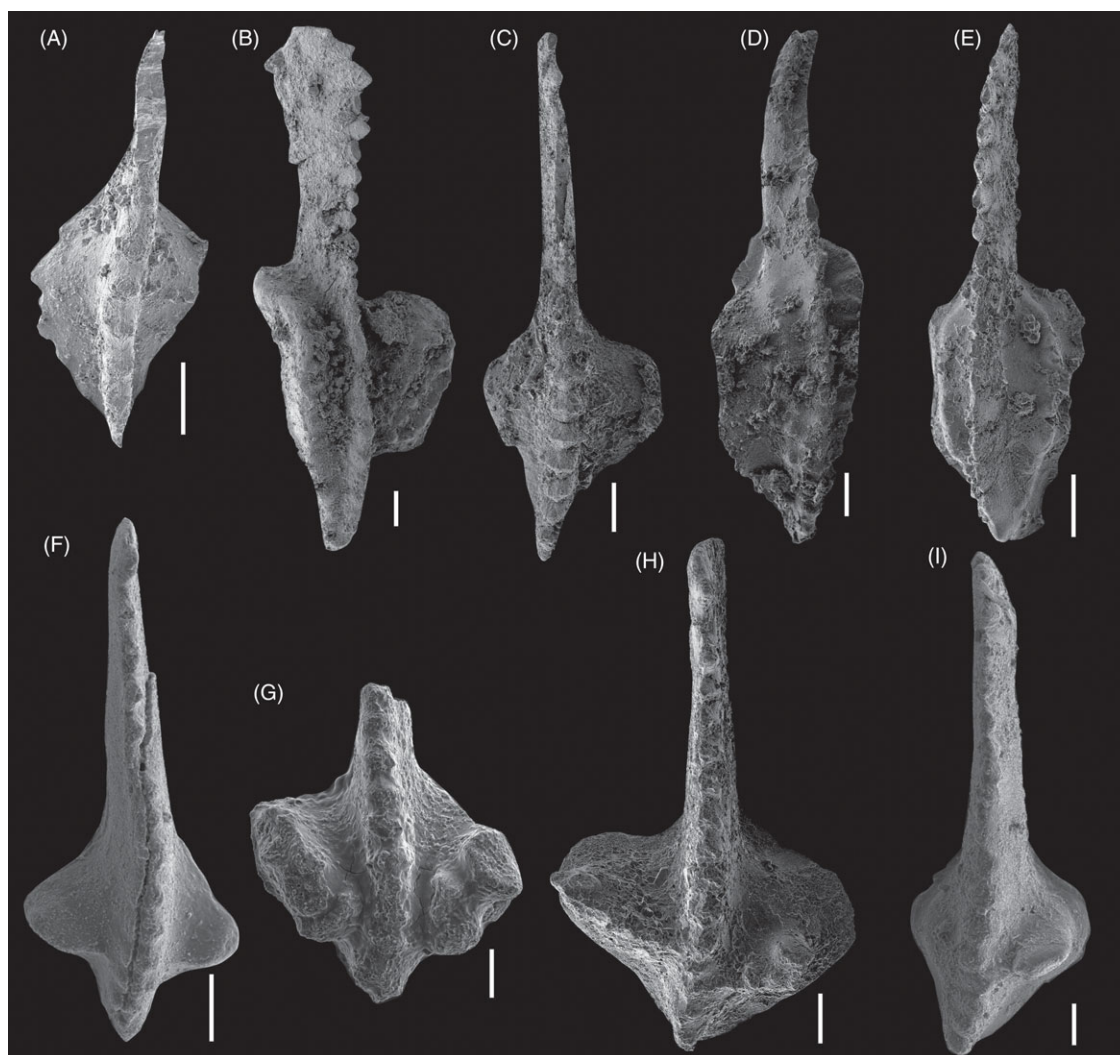
Fig. 3. Significant conodont species from the Danlu section (oral view; scale bar = 100 μm). (A) *Lochriea commutata*, DL181, 0.46 m. (B–E) DL190, 2.06 m: (B) *Gnathodus bilineatus bilineatus*; (C) *Lochriea saharae*; (D) *Gnathodus girtyi girtyi*; (E) *Pseudognathodus homopunctatus*. (F) *Lochriea costata*, DL214, 20.36 m. (G–H) *Lochriea ziegleri*. (G) DL224, 25.22 m; (H) DL226, 27.36 m. (I) *Lochriea nodosa*, DL257, 66.87 m.

(Fig. 5F). The assemblages are assigned to the lowermost upper Viséan or Aleksinian Substage (e.g. Liu *et al.* 2023) (Fig. 4).

From unit 4 to 17 (Supplemental Appendices 1–2), foraminifers are still abundant, although in less amount than those in the older levels. At sample BDL24, *Bradyina* sp., *Cribrospira* cf. *panderi* Möller and *Endothyranopsis* cf. *crassa* (Brady) occur, whereas *Eostaffella ikensis* Vissarionova (Fig. 5J) is first recorded only 3 m above. In units 7–8, oblique sections of large *Janischewskina* occur, together with '*Millerella*' *designata* Zeller (Fig. 5I), *Bradyina potanini* Venukoff (Fig. 5G) and *Asteroarchaediscus rugosus* (Rauser-Chernoussova) (Fig. 5H). This interval is assigned to the late Viséan Mikhailovian–Venevian substages (Fig. 4). Similar foraminiferal assemblages were also reported from coeval strata below the Viséan–Serpukhovian boundary elsewhere in South China, that is, in the *Bradyina* Zone of Shen & Wang (2015) and Shen *et al.* (2020) and in the lower 48 m of the Yashui section (Groves *et al.* 2012).

Janischewskina delicata (Malakhova) (Fig. 5L), *Howchinia subplana* (Brazhnikova & Yartseva) (Fig. 5M) and specimens questionably assigned to '*Millerella*' *tortula*? Zeller (Fig. 5N, O) first occur at sample BDL51 (Fig. 4). One and a half metres above,

the first *Eolasiodiscus* is recorded. The FODs of *J. delicata* and '*M.*' *tortula* have been used for the recognition of the base of the Serpukhovian in shallow-water facies (e.g. Gibshman, 2003; Groves *et al.* 2012), whereas in deeper-water facies, representatives of the family Lasiodiscidae (as *Howchinia subplana* and *Eolasiodiscus*) are usually more robust markers (Nikolaeva *et al.* 2009, 2020; Kulagina *et al.* 2011; Cózar *et al.* 2016, 2019; Vachard *et al.* 2016). This group of four taxa allows recognition of the base of the Serpukhovian from sample BDL51, at the base of unit 11.

From unit 18, foraminiferal diversity and abundance decrease notably. At sample BDL88, *Eostaffellina decurta* (Rauser-Chernoussova) (Fig. 5P) and *Endothyranopsis plana* Brazhnikova (Fig. 5Q) first occur, and 0.5 m above, *Eosigmoilina* sp. 1 (Fig. 5R) occurs (Fig. 4). *Eostaffellina decurta* is a classical marker for the Steshevian in the Russian Platform (Lipina & Reitlinger, 1971), although its first occurrence in the Tarusian is still debated (Reitlinger *et al.* 1996). In South China, it has been recorded in the latest Serpukhovian (Sheng *et al.* 2018) or close to the base of the Serpukhovian (Sheng *et al.* 2021). This taxon, however, seems to be a valid Steshevian marker in varied
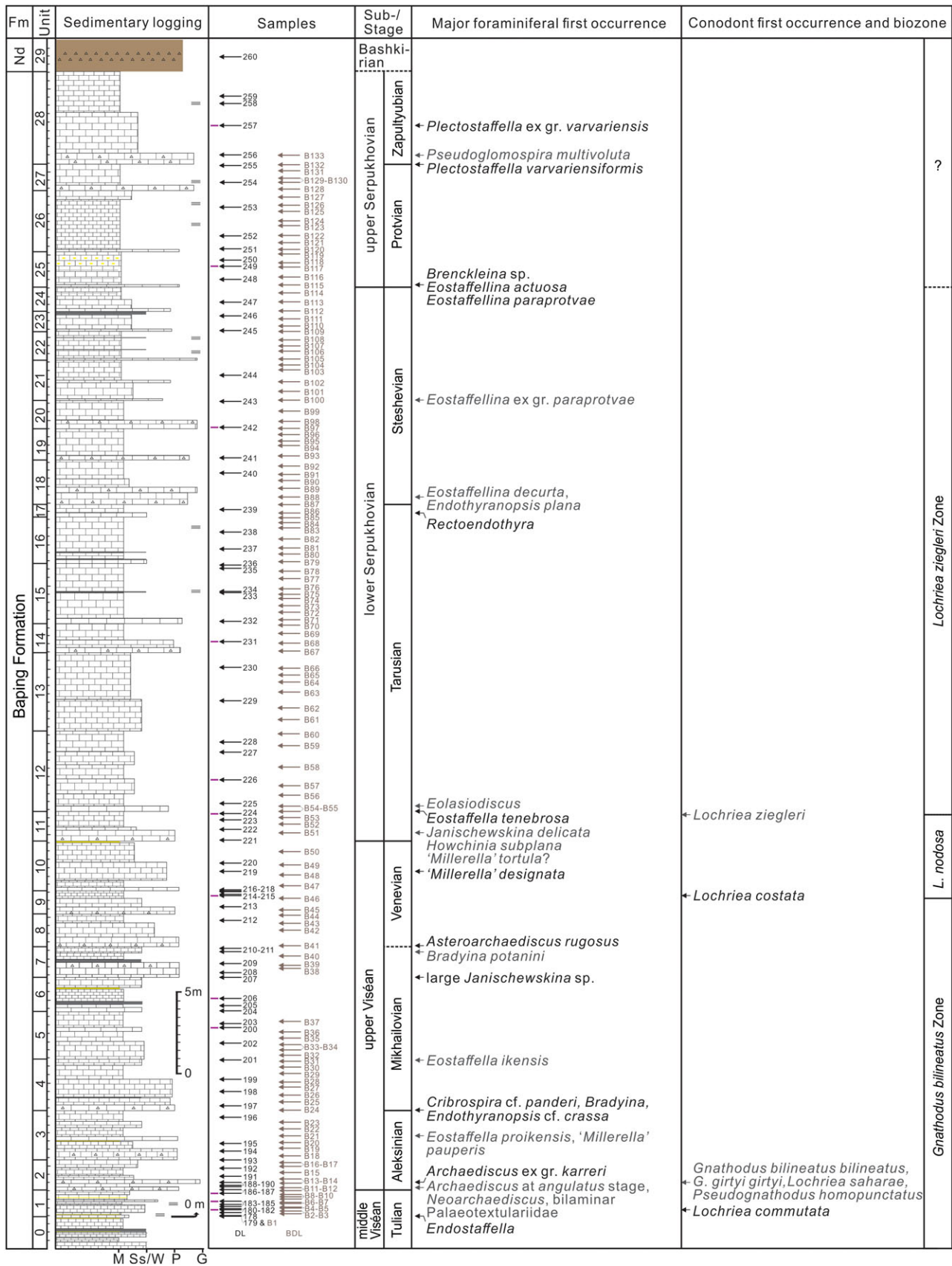
Fig. 4. (Colour online) Chronostratigraphy of the Danlu section with records of major foraminiferal and conodont first occurrences. Abbreviation: Nd, Nandan Formation.

Fig. 5. Significant foraminiferal species from the Danlu section (scale bar = 100 μm). (A–C) BDL12, 1.71 m: (A) *Archaediscus* ex gr. *karreri*; (B) *Archaediscus* at *angulatus* stage; (C) *Neoarchaediscus* aff. *parvus*. (D) *Neoarchaediscus* sp. BDL13, 2.02 m. (E–F) BDL21, 4.89 m: (E) *Eostaffella proikensis*; (F) '*Millerella*' *pauperis*. (G) *Bradyina potanini*, DL211, 17.17 m. (H) *Asteroarchaediscus rugosus*, BDL41, 17.23 m. (I) '*Millerella*' *designata*, DL219, 21.83 m. (J–K, O) BDL54, 25.37 m: (J) *Eostaffella ikensis*; (K) *Eostaffella tenebrosa*; (O) '*Millerella*' *tortula*? (L–N) BDL51, 24.20 m: (L) *Janischewskina delicata*; (M) *Howchinia subplana*; (N) '*Millerella*' *tortula*? (P–Q) BDL88, 44.47 m: (P) *Eostaffellina decurta*; (Q) *Endothyranopsis plana*. (R) *Eosigmoilina* sp. 1, BDL89, 44.97 m. (S–T) BDL100, 50.23 m, *Eostaffellina* ex gr. *paraprotvae*. (U–V) BDL115, 57.32 m: (U) *Brenckleina* sp.; (V) *Eostaffellina paraprotvae*. (W–X) *Eostaffellina actuosa*. (W) BDL 128, 63.00 m; (X) BDL115, 57.32 m. (Y) *Pseudoglomospira multivoluta*, BDL133, 65.00 m. (Z) *Plectostaffella varvariensiformis*, BDL132, 64.50 m. (AA) *Plectostaffella* ex gr. *varvariensis*, DL257, 66.87 m.

depositional settings from Western Europe (e.g. Cózar & Somerville, 2016, 2021*a*; Cózar *et al.* 2016; Vachard *et al.* 2016) and also in the Bama Platform, South China (Liu *et al.* 2023). In addition, *Endothyranopsis plana* is also documented in levels with *E. decurta* and close to *Brenckleina* (Cózar *et al.* 2016; Cózar & Somerville, 2021*a*). Hence, there are sufficient arguments to consider this part of the Danlu section as equivalent to the Steshevian (Fig. 4).

Slightly higher up in the succession, at BDL100, the first *Eostaffellina* ex gr. *paraprotvae* (Rauser-Chernoussova) (Fig. 5S, T) occurs. These narrow forms are known from the Steshevian (Gibshman *et al.* 2009; Cózar & Somerville, 2016, 2021*a*, *b*; Vachard *et al.* 2016; Liu *et al.* 2023), nearly at the same level with *Eostaffellina decurta*. Hence, this part of the section is also assigned to the Steshevian (Fig. 4).

Sample BDL115 contains the first occurrences of *Brenckleina* sp. (Fig. 5U), *Eostaffellina paraprotvae* (Fig. 5V) and *E. actuosa* Reitlinger (Fig. 5W, X). *Brenckleina* is notably recorded from the late Serpukhovian, but rarely, it has been reported from the upper part of the Steshevian (Poletaev *et al.* 1991) or in intermediate positions of

this substage from Tian Shan, England, Ireland and Spain (Kulagina *et al.* 1992; Cózar & Somerville, 2014; 2016, 2021*b*; Cózar *et al.* 2016). In contrast, *E. actuosa* is a marker for the late Serpukhovian, and this interval can be correlated with the Protvian *E. actuosa* Zone of Kulagina *et al.* (2014).

In the uppermost part of the Danlu section, below the massive dolostones, *Plectostaffella varvariensiformis* Brazhnikova & Vdovenko (Fig. 5Z), *P.* ex gr. *varvariensis* (Brazhnikova & Potievskaya) (Fig. 5AA) and common *Pseudoglomospira multivoluta* Hance, Hou and Vachard (Fig. 5Y) are first recorded (Fig. 4). This interval can be correlated with the Zapaltyubian Substage in China (Liu *et al.* 2023).

6. Evaluating the diachronism in the FODs of *Lochriea ziegleri*

6.a. Constraints from sequence stratigraphy

High-amplitude sea-level falls related to the onset of the main phases of glaciation during the LPIA have been suggested to

control the depositional architectures of tectonically stable craton basins worldwide (e.g. Smith & Read, 2000; Wright & Vanstone, 2001; Bishop *et al.* 2009; Eros *et al.* 2012; Fielding & Frank, 2015; Chen *et al.* 2019; Cózar *et al.* 2022*b*; Montañez, 2022). Hence, sequence stratigraphy in those regions should be similar, unless regional tectonics have overridden glacioeustasy and modified the patterns. Major substage boundaries have been frequently correlated (e.g. Eros *et al.* 2012), although as Cózar & Somerville (2014) and Cózar *et al.* (2018) highlighted, these glacioeustatic or onlap–offlap correlations fail when there are no solid biostratigraphic calibrations.

In the Naqing section of South China, Chen *et al.* (2016) attributed the Viséan–Serpukhovian transition to a lowstand systems tract, which was suggested to correlate with a palaeokarst with development of thick paleosols in the platform-top Yashui section. In the Danlu section, the FOD of *L. ziegleri* is at the uppermost part of a regressive systems tract (Fig. 2). To reconcile this fact, the first occurrence of *L. ziegleri* in South China is interpreted to have been accompanied by a sea-level lowstand.

In the South Urals, only transgressive–regressive sequences were recognized in the Verkhnyaya Kardailovka section (Richards *et al.* 2017). The FOD of *L. ziegleri* is located at an intermediate position of a regressive phase and the lowstand systems tract might develop in much younger strata (Richards *et al.* 2017).

In northern England, marked cyclicity in the Yoredale Series is also composed of transgressive–regressive cycles. Generally, the basal limestones represent rapid transgressions, and the overlying limestones and detrital rocks (e.g. shales, siltstones, sandstones and coals) formed in slow regressive phases, with the capped coals constituting the lowstands of the platform. Considering the FOD of *L. ziegleri* is recorded in the lower Middle Limestone (Sevastopulo & Barham, 2014), it possibly corresponds to a transgressive phase or a transgressive–regressive transition.

In the Cantabrian Mountains (NW Spain), detailed sequence stratigraphy has not been published yet, but in the Vegas de Sotres section, units 1–3 (Canalón Member, Alba Formation) can be interpreted as an overall regressive phase (Cózar *et al.* 2016), and the overlying Millaró Member is a notable drowning of the basin (Sanz-López *et al.* 2004, 2007), corresponding to a rapid transgression. As a result, the FOD of *L. ziegleri* at the uppermost unit 1 is situated in a long-term regression sequence.

In the Moscow Basin, the FOD of *L. ziegleri* coincides with a transgressive–regressive transition in the Novogurovsky section (Gibshman *et al.* 2009; Kabanov *et al.* 2016), whereas in the French Pyrenees it occurs within a long-term transgression (Perret in Skompski *et al.* 1995).

In summary, the FOD of *L. ziegleri* coincides with (i) a transgressive–regressive transition (e.g. in Northern England and Moscow Basin), (ii) a regressive phase (e.g. in the South Urals and Cantabrian Mountains), (iii) a transgression phase (e.g. in France) or (iv) a sea-level lowstand (e.g. in South China). These contrasting results do not support a synchronous first occurrence of *L. ziegleri* worldwide, although more detailed sedimentological and palaeontological studies would improve the apparent mismatches.

6.b. Constraints from the foraminifers and ammonoids

Along with searching for a more or less synchronous first occurrence of *L. ziegleri*, the number of studies on ammonoids and foraminifers from the Viséan–Serpukhovian boundary interval has also increased in the last decade, in order to determine the species

with more consistent first occurrences (e.g. Kulagina *et al.* 2019; Nikolaeva *et al.* 2020; Aleeksev *et al.* 2022). In the case of foraminifers, although facies-control problems and potential delays in the dispersion of some species around the Palaeotethys could be distinguished, a few of better markers for the Viséan–Serpukhovian boundary in outer and inner platform facies have been selected (Cózar *et al.* 2019, fig. 8). These and other previous studies have improved notably the calibration between zonal schemes of different fossil groups, allowing to clarify which species of ammonoids and foraminifers are considered as first occurring at the uppermost Viséan, at the base of the Serpukhovian or even in younger levels of this latter stage.

The Danlu section is noteworthy for the low abundance in conodonts; however, as mentioned above, the FOD of *L. ziegleri* is at sample DL224, 1.68 m above the base of the Tarusian defined with foraminifers. The occurrence of some ammonoids and foraminifers compared to *L. ziegleri* is not consistent in other basins around the world. In total, four possible scenarios or groups are observed.

6.b.1. Sections with the FOD of L. ziegleri in the Steshevian or Protvian (group 1)

Sections representative of this first group (Fig. 6) are the Kugarchi and Mariinsky sections in the Urals, Donets (Ukraine), Craven Basin in England and Kilnamona and Lugasnaghta in Ireland (Cózar & Somerville, 2021*a*).

Nikolaeva *et al.* (2017) interpreted the FOD of *L. ziegleri* in the Kugarchi section at levels equivalent to the Steshevian and attributed its absence from older levels to hostile settings. In the Mariinsky, the well-formed P1 elements of *L. ziegleri* from the base of the section make Nikolaeva *et al.* (2020) consider that its FOD should be in much lower levels. This inference explains the first occurrence of *Monotaxinoides transitorius* Brazhnikova and Yartseva, a classical marker for the Zapaltyubian in most Russian zonal schemes, only 10 m above the base, suggesting that the FOD of *L. ziegleri* might be located within the Protvian.

In Ukraine and Craven Basin in England, the first occurrence of *L. ziegleri* is also certainly late, that is, at levels close to the base of the Namurian (maybe equivalent to the uppermost Tarusian to lowermost Steshevian; Fig. 6) (Metcalfe, 1981; Skompski *et al.* 1995; Sevastopulo & Barham, 2014). However, some authors inferred its FOD within B8–B9 limestones or sequence Se-I of the Donets (Davydov *et al.* 2010; Eros *et al.* 2012), although the oldest confirmed FOD of this taxon in Ukraine is in sequence Se-VII, which probably corresponds to the Steshevian Substage (Cózar *et al.* 2019).

In Ireland, the biostratigraphy at Lugasnaghta is still debated, due to a contradiction between the ammonoid and foraminiferal records. There, *Neoarchaediscus postrugosus* (Reitlinger) and other Tarusian foraminiferal markers have been found far below the Ardvarney Limestone Member, where the P2a subzone was located (Sevastopulo & Barham, 2014). According to the ammonoids, the FOD of *L. ziegleri* would correspond to the base of the Tarusian, whereas foraminifers suggest a Steshevian Substage (Cózar & Somerville, 2021*b*). At Kilnamona, by contrast, its FOD has been well constrained to levels of the E1a subzone, within the middle part of the Steshevian (Fig. 6)

In this group of sections, as suggested by Nikolaeva *et al.* (2020), it seems to concur two problems, that is, the presence of hostile facies and the poverty in conodonts in shallow-water facies. These problems led to a certain late occurrence of *L. ziegleri*. Higher sampling effort might improve the resolution of the fossils in those regions.
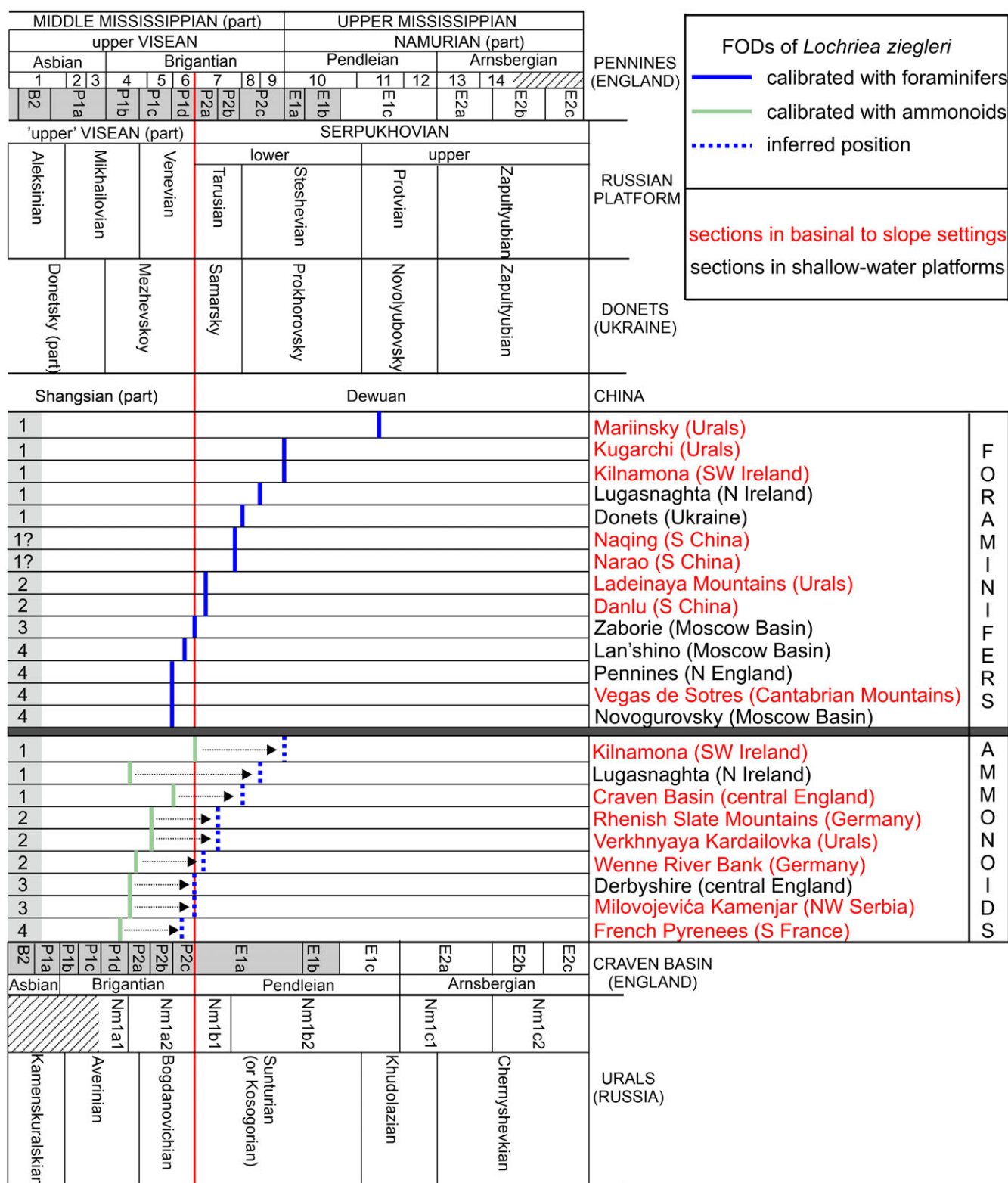
Fig. 6. (Colour online) FODs of *Lochriea ziegleri* in different basins. In the upper part, Pennines (England) chronostratigraphy, foraminiferal zones (1–14; Cózar & Somerville, 2021*a*) and their correlations with the ammonoid zones in shallow-water platforms of England (B2 to E2c) are included. In the lower part, the Urals chronostratigraphy is compared with that of the basinal Craven Basin (England) and the regional ammonoid zones proposed by Nikolaeva (2013). Note the different correlation of the ammonoid zones from England below the E1c subzone using the calibration of foraminifers in the Pennines and the ammonoids from the Urals (grey areas in Craven and Pennines). Inferred position corresponds to the recognized ammonoid zones using the calibration in the Pennines.

The Narao and Naqing sections from South China might be also incorporated in this group, but its biostratigraphy has not been sufficiently constrained yet. In the Naqing section, only scarce foraminiferal representatives are present (Groves *et al.* 2012). Although Sheng (2017) and Wang *et al.* (2017) mentioned that *Janischewskina delicata* and *Bradyina* aff. *cribrostomata* Rauser-Chernoussova & Reitlinger are recorded at 2.15 and 2.20 m above the FOD of *L. ziegleri*, respectively, none of the species were illustrated. As discussed in Cózar *et al.* (2019), the occurrence of *B.* aff. *cribrostomata* close to the base of the Serpukhovian is unusual. The oldest record of *B. cribrostomata* in the literature seems to be at the uppermost lower Serpukhovian (Aizenverg *et al.* 1983; Cózar & Somerville, 2021*a*), whereas a more common occurrence is in the upper Serpukhovian (Conil *et al.* 1991; Reitlinger *et al.* 1996; Cózar *et al.* 2011). In the Fenghuangshan section, this species was selected as the nominal taxon for the *B. cribrostomata* Zone, representative of the late Serpukhovian Protvian Substage (Sheng *et al.* 2018). Similarly, foraminiferal biostratigraphy from the Bama Platform, Youjiang Basin, suggests that *B. cribrostomata* is first recorded from levels equivalent to the uppermost Steshevian (Liu *et al.* 2023). On the other hand, the Narao section records the first *J. delicata* ca. 2.2 m above the FOD of *L. ziegleri* (Sheng *et al.* 2021). However, the specimen was obtained from a thick conglomerate, and thus, reworking can be assumed. The illustrated *Eostaffellina decurta* ca. 4.0 m above the FOD of *L. ziegleri* (Sheng *et al.* 2021) is one of typical narrow and small forms attributed here to *Eostaffellina* ex gr. *paraprotvae* (compared with Fig. 5S), which, similar to the Danlu section, in the shallow-water Bama Platform, first occurs in the Steshevian (Liu *et al.* 2023). In consequence, the close entry of *L. ziegleri* to *B.* aff. *cribrostomata* and *Eostaffellina* ex gr. *paraprotvae* suggests that the first *L. ziegleri* might occur later in these two sections, likely corresponding to slightly higher levels in the Tarusian, or even in the Steshevian (Fig. 6).

6.b.2. Sections with the FOD of L. ziegleri *slightly above the base of the Serpukhovian (group 2)*

Among the second group of sections, taking into consideration the problems with the ammonoid biostratigraphic correlations (e.g. Nikolaeva & Kullmann, 2001; Nikolaeva 2013), the FODs of *L. ziegleri* seem to be above the basal P2a subzone (Fig. 6), and thus, above the level equivalent to the base of the Tarusian in the Pennines. Such cases include the Rhenish Slate Mountains and Wenne River bank sections in Germany (Skompski *et al.* 1995; Wang *et al.* 2018), the Ladeinaya Mountains and Verkhnyaya Kardailovka in the Urals (Nikolaeva *et al.* 2009, 2020; Richards *et al.* 2017) and the Danlu section.

Nemyrovskaya *et al.* (1994) previously considered the FOD of *L. ziegleri* in the Rhenish Slate Mountains in the P1d subzone, but a revision by Herbig (2017) and Herbig *et al.* (2017) indicated that it could not be confirmed an older FOD of *L. ziegleri* below the P2b subzone (= upper Tarusian; Fig. 6). Thus, the FOD of *L. ziegleri* in this region of Germany is still pending of confirmation (Sevastopulo & Barham, 2014).

The slight delay of the FOD of *L. ziegleri* in the Ladeinaya Mountains and Danlu sections could be attributed to the poverty in conodonts, due to their relatively shallower-water settings than others, which explains the richest foraminiferal assemblages, as well as the common occurrence of foraminifers predominantly from shallow-water platforms. Alternatively, this delay might result from hostile facies (i.e. cherty and bituminous beds).

The delay observed in the Wenne River Bank and Verkhnyaya Kardailovka sections (Fig. 6) might be related to the mismatch in the correlation of the ammonoid zones recognized from the basinal facies (e.g. Craven Basin) and shallow-water platforms (e.g. Pennines), with these latter zones calibrated with foraminiferal zones defined in other regions (e.g. the Moscow Basin). Hence, this apparent late occurrence of *L. ziegleri* might be an artefact generated by incorrect ammonoid-foraminiferal zonal calibrations.

6.b.3. Sections with the FOD of L. ziegleri *coinciding with the base of the Serpukhovian (group 3)*

In some sections (the third group), the FOD of *L. ziegleri* coincides with the base of the P2a subzone or the base of the Tarusian, such as the Milivojevića Kamenjar section in Serbia (Sudar *et al.* 2018), Derbyshire in England (Higgins, 1975) and Zaborie in Russia (Kabanov *et al.* 2009).

In the Zaborie Quarry, it is difficult to obtain older records of *L. ziegleri*, because there are only two beds assigned to the Venevian, and currently, only bed 2 is exposed (Kabanov *et al.* 2009). Thus, the absence of older *L. ziegleri* might be an artefact due to the nearly absence of Venevian strata (mostly covered).

In Derbyshire, the FOD of *L. ziegleri* coincides with a major lithological change, from the Eyam Limestone (bioclastic shallow-water limestones and reefs) to the Widmerpool (deep-water mudstones and shales) formations. Thus, the occurrence of the conodont from the latter formation might be a matter of facies control. A similar scenario is also observed in the Milivojevića Kamenjar section, where nearly all the ornamented *Lochriea* first occur together in less than 1 m of strata, with a major lithological change from light-grey thick-bedded to massive micritic limestones passing into well-bedded nodular micritic limestones (Sudar *et al.* 2018).

6.b.4. Sections with the FOD of L. ziegleri *in slightly older levels than the base of the Serpukhovian (group 4)*

In a final fourth group of sections, the FODs of *L. ziegleri* coincide with the P1d subzone or intermediate levels in the Venevian, including the successions from the southern Pennines in northern England (Varker in Skompski *et al.* 1995), the French Pyrenees (Perret in Skompski *et al.* 1995), the Novogurovsky and Lan'shino sections in the Moscow Basin (Alekseev in Skompski *et al.* 1995; Gibshman *et al.* 2009) and the Vegas de Sotres section in NW Spain (Cózar *et al.* 2016) (Fig. 6).

Only these sections agree with the inferred FAD of *L. ziegleri* in levels slightly older than the current base of the Serpukhovian, the requirement suggested by Richards & Task Group (2005) to be a reliable marker for the Viséan–Serpukhovian boundary. Nevertheless, for the groups 1–3, although there are some reasonable explanations to justify a possible delay in the FOD of *L. ziegleri* in some of the sections, in general, they suggest a lack of synchronicity (Fig. 6).

It can be inferred that further studies are necessary to clarify the above-described problems, including more intensive samplings for foraminifers, conodonts and ammonoids in those sections where some discrepancies have been observed.

7. Conclusions

Sequence stratigraphy, foraminifers and conodonts of the Baping Formation in the carbonate-slope Danlu section, Youjiang Basin, allow to constrain the stratigraphical context and the FOD of the conodont *Lochriea ziegleri* with potential foraminiferal markers

near the Viséan–Serpukhovian boundary in China. The apparent delays in the FODs of *L. ziegleri* in some basins and the problems in its calibration caused by the use of different fossil groups, zonal schemes and indirect correlations demonstrate that the assumed synchronous FAD of the conodont cannot be confirmed. In addition to a lack of synchronicity, independently evidenced by distinct sequence stratigraphic contexts, some apparent later occurrences might be also in part due to poor calibrations between deep- and shallow-water zonal schemes, as well as the frequent presence of favourable or hostile facies for conodonts. Some of those problems have not been investigated sufficiently or are currently in progress. Therefore, it is recommended that more parameters should be investigated for the recognition of a new base for the Serpukhovian, as well as to achieve a far better correlation between different zonal schemes and fossil groups.

References

Aizenverg DE, Astakhova TV, Berchenko OI, Brazhnikova NE, Vdovenko MV, Dunaeva NN, Zernetskaya NV, Poletaev VI and Sergeeva MT (1983) *Late Serpukhovian substage in the Donets Basin.* Kiev: Akademiya Nauk Ukrainskoi SSR, Institut Geologicheskii Nauk, 164 p. (in Russian).

Alekseev AS, Nikolaeva SV, Goreva NV, Donova NB, Kossovaya OL, Kulagina EI, Kucheva NA, Kurilenko AV, Kutygin RV, Popeko LI and Stepanova TI (2022) Russian regional Carboniferous stratigraphy. In *The Carboniferous Timescale* (eds SG Lucas, JW Schneider, X Wang and S Nikolaeva), pp. 49–117. London: Geological Society, Special Publications 512.

Barham M, Murray J, Sevastopulo GD and Williams DM (2015) Conodonts of the genus *Lochriea* in Ireland and the recognition of the Viséan-Serpukhovian (Carboniferous) boundary. *Lethaia* **48**, 151–71.

Bishop JW, Montañez IP, Gulbranson EL and Brenckle PL (2009) The onset of mid-Carboniferous glacio-eustasy: sedimentologic and diagenetic constraints, Arrow Canyon, Nevada. *Palaeogeography, Palaeoclimatology, Palaeoecology* **276**, 217–43.

Chen J, Montañez IP, Qi Y, Wang X, Wang Q and Lin W (2016) Coupled sedimentary and δ13C records of late Mississippian platform-to-slope successions from South China: insight into δ13C chemostratigraphy. *Palaeogeography, Palaeoclimatology, Palaeoecology* **448**, 162–78.

Chen J, Sheng Q, Hu K, Yao L, Lin W, Montañez IP, Tian X, Qi Y and Wang X (2019) Late Mississippian glacio-eustasy recorded in the eastern Paleo-Tethys Ocean (South China). *Palaeogeography, Palaeoclimatology, Palaeoecology* **531**, 108873.

Conil R, Groessens E, Laloux M, Poty E and Tourneur F (1991) Carboniferous guide foraminifera, corals and conodonts in the Franco-Belgian and Campine basins. Their potential for widespread correlation. *Courier Forschungsinstitut Senckenberg* **130**, 15–30.

Cózar P, Somerville ID, Blanco-Ferrera S and Sanz-López J (2018) Palaeobiogeographical context in the development of shallow-water late Viséan-early Bashkirian benthic foraminifers and calcareous algae in the Cantabrian Mountains (Spain). *Palaeogeography, Palaeoclimatology, Palaeoecology* **551**, 620–38.

Cózar P and Somerville ID (2014) Latest Viséan-Early Namurian (Carboniferous) foraminifers from Britain: implications for biostratigraphic and glacioeustatic correlations. *Newsletters on Stratigraphy* **47**, 355–67.

Cózar P and Somerville ID (2016) Problems correlating the late Brigantian–Arnsbergian Western European substages within northern England. *Geological Journal* **51**, 817–40.

Cózar P and Somerville ID (2021a) The Serpukhovian in Britain: use of foraminiferal assemblages for dating and correlating. *Journal of the Geological Society, London* **178**, jgs2020-170.

Cózar P and Somerville ID (2021b) Irish Serpukhovian revisited. *Geological Journal* **56**, 1403–23.

Cózar P, Said I, Somerville ID, Vachard D, Medina-Varea P, Rodríguez S and Berkhli M (2011) Potential foraminiferal markers for the Viséan-Serpukhovian and Serpukhovian-Bashkirian boundaries——— a case-study from central Morocco. *Journal of Paleontology* **85**, 1105–27.

Cózar P, Somerville ID and Hounslow MW (2022a) Foraminifers in the Holkerian Stratotype, regional substage in Britain: key taxa for the Viséan subdivision. *Newsletters on Stratigraphy* **55**, 159–172.

Cózar P, Somerville ID, Hounslow MW and Coronado I (2022b) Far-field correlation of palaeokarstic surfaces in Mississippian successions using high-frequency foraminiferal diversity trends. *Palaeogeography, Palaeoclimatology, Palaeoecology* **601**, 111088.

Cózar P, Somerville ID, Sanz-López J and Blanco-Ferrera S (2016) Foraminiferal biostratigraphy across the Visean/Serpukhovian boundary in the Vegas de Sotres section (Cantabrian Mountains, Spain). *Journal of Foraminiferal Research* **46**, 171–92.

Cózar P, Vachard D, Aretz M and Somerville ID (2019) Foraminifers of the Viséan-Serpukhovian boundary interval in Western Palaeotethys: a review. *Lethaia* **52**, 260–84.

Davydov VI and Cózar P (2019) The formation of the Alleghenian Isthmus triggered the Bashkirian glaciation: constraints from warm-water benthic foraminifera. *Palaeogeography, Palaeoclimatology, Palaeoecology* **531**, 108403.

Davydov VI, Crowley JL, Schmitz MD and Poletaev VI (2010) High-precision U-Pb zircon age calibration of the global Carboniferous time scale and Milankovitch band cyclicity in the Donets basin, eastern Ukraine. *Geochemistry, Geophysics, Geosystems* **11**, Q0AA04.

Du Y, Huang H, Yang J, Huang H, Tao P, Huang Z, Hu L and Xie C (2013) The basin translation from Late Paleozoic to Triassic of the Youjiang Basin and its tectonic signification. *Geological Review* **59**, 1–11 (in Chinese with English abstract).

Eros JM, Montañez LP, Osleger DA, Davydov VI, Nemyrovska TI, Poletaev VI and Zhykalyak MV (2012) Sequence stratigraphy and onlap history of the Donets Basin, Ukraine: insight into Carboniferous icehouse dynamics. *Palaeogeography, Palaeoclimatology, Palaeoecology* **313–314**, 1–25.

Fielding CR and Frank TD (2015) Onset of the glacioeustatic signal recording late Palaeozoic Gondwanan ice growth: new data from palaeotropical East Fife, Scotland. *Palaeogeography, Palaeoclimatology, Palaeoecology* **426**, 121–38.

Fielding CR, Frank TD, Birgenheier LP, Rygel MC, Jones AT and Roberts J (2008) Stratigraphic imprint of the Late Palaeozoic Ice Age in eastern Australia: a record of alternating glacial and nonglacial climate regime. *Journal of the Geological Society* **165**, 129–40.

Gibshman NB (2003) Foraminifers from the Serpukhovian Stage stratotype, the Zabor'e Quarry site (Moscow region). *Stratigraphy and Geological Correlation* **11**, 36–60.

Gibshman NB, Kabanov PB, Alekseev AS, Goreva NV and Moshkina MA (2009) Novogurovsky Quarry—Upper Visean and Serpukhovian. In *Type and reference Carboniferous sections in the south part of the Moscow Basin. Field Trip Guidebook of International Field Meeting of the I.U.G.S. Subcommission on Carboniferous Stratigraphy* (eds AS Alekseev and NN Goreva), pp. 13–44. Moscow: Borissiak Paleontological Institute of Russian Academy of Sciences.

Groves JR, Wang Y, Qi Y, Richards BC, Ueno K and Wang X (2012) Foraminiferal biostratigraphy of the Visean–Serpukhovian (Mississippian) boundary interval at slope and platform sections in southern Guizhou (South China). *Journal of Paleontology* **86**, 753–74.

Herbig H-G (2017) Taxomomic and stratigraphic problems concerning the conodont Lochriea senckenbergica Nemirovskaya, Perret & Meischner, 1994 and Lochriea ziegleri Nemirovskaya, Perret & Meischner, 1994 - consequence for defining the Viséan-Serpukhovian boundary. *Newsletter on Carboniferous Stratigraphy* **33**, 28–35.

Herbig H-G, Bätz S and Resag K (2017) A potential conodont-based Viséan-Serpukhovian boundary – data from the Rhenish Mountains (Germany). In *International Conference "Uppermost Devonian and Carboniferous carbonate buildups and boundary stratotypes". Abstracts and papers of International Field Meeting of the I.U.G.S. Subcommission on Carboniferous Stratigraphy* (eds GZ Zholtaev, VY Zhaimina, EM Fazylov, SV Nikolaeva and ES Musina), pp. 25–32. Almaty, Turkestan, August 15–22, 2017.

Higgins AC (1975) Conodont zonation of the Late Visean and Early Westphalian strata of the south and central Pennines of northern England. *Bulletin of the Geological Survey of Great Britain* **53**, 1–90.

Hu K, Qi Y, Qie W and Wang Q (2020) Carboniferous conodont zonation of China. *Newsletters on Stratigraphy* **53**, 141–90.

Kabanov PB, Alekseev AS, Gibshman NB, Gabdullin RR and Bershov AV (2016) The upper Viséan–Serpukhovian in the type area for the Serpukhovian Stage (Moscow Basin, Russia): part 1. Sequences, disconformities, and biostratigraphic summary. *Geological Journal* **51**, 163–94.

Kabanov PB, Gibshman NB, Barskov IS, Alekseev AS and Goreva NV (2009) Zaborie Section—Lectostratotype of Serpukhovian Stage. In *Type and reference Carboniferous sections in the south part of the Moscow Basin. Field Trip Guidebook of International Field Meeting of the I.U.G.S. Subcommission on Carboniferous Stratigraphy* (eds AS Alekseev and NN Goreva), pp. 45–64. Moscow: Borissiak Paleontological Institute of Russian Academy of Sciences.

Korn D, Titus AL, Ebbighausen V, Mapes RH and Sudar MN (2012) Early Carboniferous (Mississippian) ammonoid biogeography. *Geobios* **45**, 67–77.

Kulagina EI, Gorozhanina EN, Gorozhanin VM and Filimonova TV (2019) Upper Viséan and Serpukhovian Biostratigraphy and Lithofacies of the Southeast of the East European Platform. *Stratigraphy and Geological Correlation* **27**, 613–37.

Kulagina EI, Nikolaeva S, Pazukhin V and Kochetova N (2014) Biostratigraphy and lithostratigraphy of the Mid-Carboniferous boundary beds in the Muradymovo section (South Urals, Russia). *Geological Magazine* **151**, 269–98.

Kulagina EI, Rumyantseva ZS, Pazukhin VN and Kochetova NN (1992) *Lower/Middle Carboniferous boundary in the South Urals and Central Tien Shan*. Moscow: Publishing Office "Nauka", 112 p. (in Russian).

Kulagina EI, Stepanova TI, Kucheva NA and Nikolaeva SV (2011) The Viséan-Serpukhovian boundary on the eastern slope of the South Urals. *Newsletter on Carboniferous Stratigraphy* **29**, 50–6.

Lantzsch H, Roth S, Reijmer JJG and Kinkel H (2007) Sea-level related resedimentation processes on the northern slope of Little Bahama Bank (Middle Pleistocene to Holocene). *Sedimentology* **54**, 1307–22.

Lipina OA and Reitlinger EA (1971) Stratigraphie zonale et paléozoogéographie du Carbonifère Inférieur d'après les foraminifères. In VI Congrès International du Carbonifère, Comptes Rendus 3, pp. 1101–1112. The University of Sheffield.

Liu B and Xu X (1994) *Lithofacies Paleogeographic Atlas of South China: Sinian–Triassic*. Beijing: Science Press, pp. 1118–1119 (in Chinese).

Liu C, Jarochowska E, Du Y, Vachard D and Munnecke A (2015) Microfacies and carbon isotope records of Mississippian carbonates from the isolated Bama Platform of Youjiang Basin, South China: possible responses to climate-driven upwelling. *Palaeogeography, Palaeoclimatology, Palaeoecology* **438**, 96–112.

Liu C, Vachard D, Cózar P and Coronado I (2023) Middle to Late Mississippian and Early Pennsylvanian foraminiferal zonal scheme of South China —— a case study from the Youjiang Basin: biostratigraphic and palaeobiogeographic implications. *Lethaia* **56**, 1–23.

Metcalfe I (1981) Conodont zonation and correlation of the Dinantian and early Namurian strata of the Craven lowlands of Northern England. *Report of the Institute of Geological Sciences* 80/10, 1–70.

Montañez IP and Poulsen CJ (2013) The late paleozoic ice age: an evolving paradigm. *Annual Review of Earth and Planetary Sciences* **41**, 629–56.

Montañez IP (2022) Current synthesis of the penultimate icehouse and its imprint on the Upper Devonian through Permian stratigraphic record. *Geological Society, London, Special Publications* **512**, 213–45.

Nemirovskaya T, Perret MF and Meischner D (1994) Lochriea ziegleri and Lochriea senckenbergica – new conodont species from the latest Viséan and Serpukhovian in Europe. *Courier Forschungsinstitut Senckenberg* **168**, 311–7.

Nikolaeva S and Kullmann J (2001) Problems in lower Serpukhovian ammonoid biostratigraphy. *Newsletter on Carboniferous Stratigraphy* **19**, 35–7.

Nikolaeva SV (2013) New Viséan and Serpukhovian ammonoids from the Verkhanyaya Kardailovka Section, eastern slope of the South Urals. *Paleontological Journal* **47**, 386–99.

Nikolaeva SV, Alekseev AS, Kulagina EI, Gatovsky YA, Ponomareva GY and Gibshman NB (2020) An evaluation of biostratigraphic markers across multiple geological sections in the search for the GSSP of the base of the Serpukhovian Stage (Mississippian). *Palaeoworld* **29**, 270–302.

Nikolaeva SV, Kulagina EI, Gorozhanina EN, Alekseev AS and Konovalova VA (2017) Conodonts, ammonoids, foraminifers, and depositional settings of the Serpukhovian and Bashkirian in the Kugarchi section in the South Urals. *Stratigraphy* **14**, 319–47.

Nikolaeva SV, Kulagina EI, Pazukhin N, Kochetova NN and Konvalova A (2009) Paleontology and microfacies of the Serpukhovian in the Verkhnyaya Kardailovka section, south Urals, Russia: potential candidate for the GSSP for the Viséan-Serpukhovian boundary. *Newsletters on Stratigraphy* **43**, 165–93.

Poletaev I, Brazhnikova NE, Vasilyuk NP and Vdovenko MV (1991) Local zones and major Lower Carboniferous biostratigraphic boundaries of the Donets Basin (Donbass). *Courier Forschungsinstitut Senckenberg* **130**, 47–50.

Qi Y, Hu K, Wang Q and Lin W (2014a) Carboniferous conodont biostratigraphy of the Dianzishang section, Zhenning, Guizhou, South China. *Geological Magazine* **151**, 311–27.

Qi Y, Nemyrovska TI, Wang Q, Hu K, Wang X and Lane HR (2018) Conodonts of the genus Lochriea near the Visean–Serpukhovian boundary (Mississippian) at the Naqing section, Guizhou Province, South China. *Palaeoworld* **27**, 423–37.

Qi Y, Nemyrovska TI, Wang X, Chen J, Wang Z, Lane HR, Richards BC, Hu K and Wang Q (2014b) Late Visean–early Serpukhovian conodont succession at the Naqing (Nashui) section in Guizhou, South China. *Geological Magazine* **151**, 254–68.

Reijmer JJG, Palmieri P and Groen R (2012) Compositional variations in calciturbidites and calcidebrites in response to sea-level fluctuations (Exuma Sound, Bahamas). *Facies* **58**, 493–507.

Reitlinger EA, Vdovenko MV, Gubareva VS and Shcherbakov OA (1996) European part of the USSR: Lower Carboniferous. In *The Carboniferous of the World III, The Former USSR, Mongolia, Middle Eastern Platform, Afghanistan and Iran* (eds RH Wagner, CF Winkler Prins and LF Granados), pp. 23–54. Madrid: Instituto Geológico y Minero de España/ Nationaal Natuurhistorisch Museum, IUGS Publication No. 33.

Richards BC and Task Group (2003) Progress report from the Task Group to establish a GSSP close to the existing Visean–Serpukhovian boundary. *Newsletter on Carboniferous Stratigraphy* **21**, 6–10.

Richards BC and Task Group (2005) The Viséan-Serpukhovian boundary: a summary of progress made on research goals established at the XV-ICCP Carboniferous Workshop in Utrecht. *Newsletter on Carboniferous Stratigraphy* **23**, 7–8.

Richards BC and Task Group (2014) Report of the Task Group to establish a GSSP close to the existing Viséan–Serpukhovian boundary. *Newsletter on Carboniferous Stratigraphy* **31**, 29–33.

Richards BC (2013) Current status of the international Carboniferous time scale. *The Carboniferous–Permian Transition, Bulletin* **60**, 348–53.

Richards BC, Nikolaeva SV, Kulagina EI, Alekseev AS, Gorozhanina EN, Gorozhanin VM, Konovalova VA, Goreva NV, Joachimski MM and

Gatovsky YA (2017) A candidate for the Global Stratotype Section and Point at the base of the Serpukhovian in the South Urals, Russia. *Stratigraphy and Geological Correlation* **25**, 697–758.

Sanz-López J, Blanco-Ferrera S and Sánchez de Posada LC (2004) Estratigrafía del Serpukhoviense y el Bashkiriense inferior (Carbonífero) en la provincia de Pliegues y Mantos Zona Cantábrica. *Geo-Temas* **6**, 131–4.

Sanz-López J, Blanco-Ferrera S, Sánchez de Posada LC and García-López S (2007) Serpukhovian conodonts from northern Spain and their biostratigraphic application. *Palaeontology* **50**, 883–904.

Scotese CR (2021) An atlas of Phanerozoic paleogeographic maps: the seas come in and the seas go out. *Annual Review of Earth and Planetary Sciences* **49**, 679–728.

Sevastopulo GD and Barham M (2014) Correlation of the base of the Serpukhovian Stage (Mississippian) in NW Europe. *Geological Magazine* **151**, 244–53.

Shen Y and Wang X (2015) Foraminiferal biostratigraphy of the Bei'an Formation (Visean–Serpukhovian) in the Pengchong area of Liuzhou, Guangxi, South China. *Alcheringa: An Australasian Journal of Palaeontology* **39**, 559–72.

Shen Y, Wang X, Li Y, Yang Z, Cen W and Wang X (2020) Carboniferous foraminifers from the Shangsi area in southern Guizhou and the Visean foraminiferal succession in South China. *Earth Science Frontiers* **27**, 213–33 (in Chinese with English abstract).

Sheng Q (2017) Mississippian foraminifers from South China. Geological Society of America Annual Meeting, Seattle, Washington, October 2017, Abstracts, 378–2.

Sheng Q, Wang Q, Qi Y and Liao Z (2021) Foraminifers around the Viséan-Serpukhovian boundary at the Narao section, Guizhou Province. *Journal of Stratigraphy* **45**, 1–10 (in Chinese with English abstract).

Sheng Q, Wang X, Brenckle P and Huber BT (2018) Serpukhovian (Mississippian) foraminiferal zones from the Fenghuangshan section,

Anhui Province, South China: implications for biostratigraphic correlations. *Geological Journal* **53**, 45–57.

Skompski S, Alekseev A, Meischner D, Nemyrovska T, Perret MF and Varker WJ (1995) Conodont distribution across the Viséan/Namurian boundary. *Courier Forschungsinstitut Senckenberg* **188**, 183–206.

Smith LB and Read JF (2000) Rapid onset of late Paleozoic glaciation on Gondwana: evidence from Upper Mississippian strata of the Mid-continent, United States. *Geology* **28**, 279–82.

Sudar MN, Novak M, Korn D and Jovanović D (2018) Conodont biostratigraphy and microfacies of the Late Devonian to Early Carboniferous Milivojevića Kamenjar section (Drůzetić, NW Serbia). *Bulletin of Geosciences* **93**, 163–83.

Vachard D, Cózar P, Aretz M and Izart A (2016) Late Viséan-early Serpukhovian foraminifers in the Montagne Noire (France): biostratigraphic revision and correlation with the Russian substages. *Geobios* **49**, 469–98.

Wang Q, Korn D, Nemyrovska T and Qi Y (2018) The Wenne riverbank section — an excellent section for the Viséan–Serpukhovian boundary based on conodonts and ammonoids (Mississippian; Rhenish Mountains, Germany). *Newsletters on Stratigraphy* **51**, 427–44.

Wang Q, Qi Y, Hu K, Sheng Q and Lin W (2014) Conodont biostratigraphy of the Visean-Serpukhovian boundary interval in the Luokun section, Luodian, Guizhou, South China. *Journal of Stratigraphy* **38**, 277–89 (in Chinese with English abstract).

Wang Q, Qi Y, Korn D, Chen J, Sheng Q and Nemyrovska T (2017) Progress on the Viséan-Serpukhovian boundary in South China and Germany. *Newsletter on Carboniferous Stratigraphy* **33**, 35–42.

Wang X, Qie W, Sheng Q, Qi Y, Wang Y, Liao Z, Shen S and Ueno K (2013) Carboniferous and Lower Permian sedimentological cycles and biotic events of South China. *Geological Society, London, Special Publications* **376**, 33–46.

Wright VP and Vanstone SD (2001) Onset of Late Palaeozoic glacio-eustasy and the evolving climates of low latitude areas: a synthesis of current understanding. *Journal of the Geological Society* **158**, 579–82.